Measurements and simulations of the ionic wind produced by a DC corona discharge between cylindrical wires

P. Bérard, D.A. Lacoste and C.O. Laux
Laboratoire EM2C, CNRS UPR 288, École Centrale Paris,
Grande Voie des Vignes, 92290 Châtenay-Malabry, France

Abstract
A parametric study of the ionic wind produced by a DC corona between two parallel wires in atmospheric air is presented. The experiment intends to examine the effect of the gap distance between the electrodes, the wire diameters, the material and the polarity of the electrodes, the voltage and the current. The current is steady for the positive discharge and pulsed (Trichel pulses) in the negative one. The state of the surface of the electrodes (but not their material) does have an effect on the ionic wind. We verified the analytic prediction that the ionic wind varies as the square root of the current. In our experimental ranges, to maximize the ionic wind, the distance must be the smallest, the electrode diameter dissymmetry the largest. A model is proposed to simulate the ionic wind for our experimental setup. The results with simplified air chemistry are in good agreement with the measurements.

1. Introduction

The effect of the ionic wind created by a corona discharge or a dielectric barrier discharge on the boundary layer of an airfoil has interesting potential applications for the purpose of reducing drag, controlling the transition to turbulence, and for flow actuation. Léger *et al.* [1], Roth *et al.* [2], and Corke *et al.* [3], have successfully demonstrated boundary layer reattachment of a low-speed flow on a surface. Predictions of the ionic wind between two wires have been made with analytical models (Stuetzer [4]) and more recently with numerical simulation (Matéo-Vélez *et al.* [6]). However there are no clear and conclusive comparisons at present between experiments and simulations for the wire-wire geometry in air. Furthermore, the velocities presently reached are too small to be applicable in high-speed flows. Thus, we propose a parametric study of a simple test case composed of two wires to quantify the effect of the discharge and the geometry on the flow velocity.
The principle of the ionic wind between two wires can be explained as follows (Lacoste *et al.* [9]). Around each wire, the electric field decreases inversely proportional to the distance to the wire. For small wire diameters, the electric field is high enough to ionize the air. The positive ions drift toward the cathode while the negative ions stay close to the anode. In their movement, the positive ions collide with the neutral molecules and transfer momentum. At the vicinity of the cathode, electrons attach to oxygen and O_2^- drifts toward the anode, transferring momentum to the neutrals. Two opposite charge currents appear. The net flow is called the ionic wind.

2. Experimental setup

The experimental setup, shown in Figure 1, is comprised of two parallel wires of 20 cm length in air at atmospheric pressure and ambient temperature. The adjustable parameters are the diameter, material, and polarity of the electrodes, as well as the gap distance, the voltage, and the current. Electrodes of various materials (copper, steel, zonc, aluminium) and diameters (from 0.2 to 1.0 mm for the first wire and from 1.0 to 2.0 mm for the second) can be used. The gap between the two wires is adjustable from 0.5 to 4 cm. The thinnest electrode is raised to a high DC potential adjustable up to 20 kV with a FUG 140-20000 power supply. The other one is connected to ground. We measured the current-voltage characteristics and the flow velocities (using Laser Doppler Velocimetry), as a function of the various parameters. All velocities presented in this paper were measured in the middle of the gap. All results presented here were obtained with the positively stressed electrode in quiescent air.

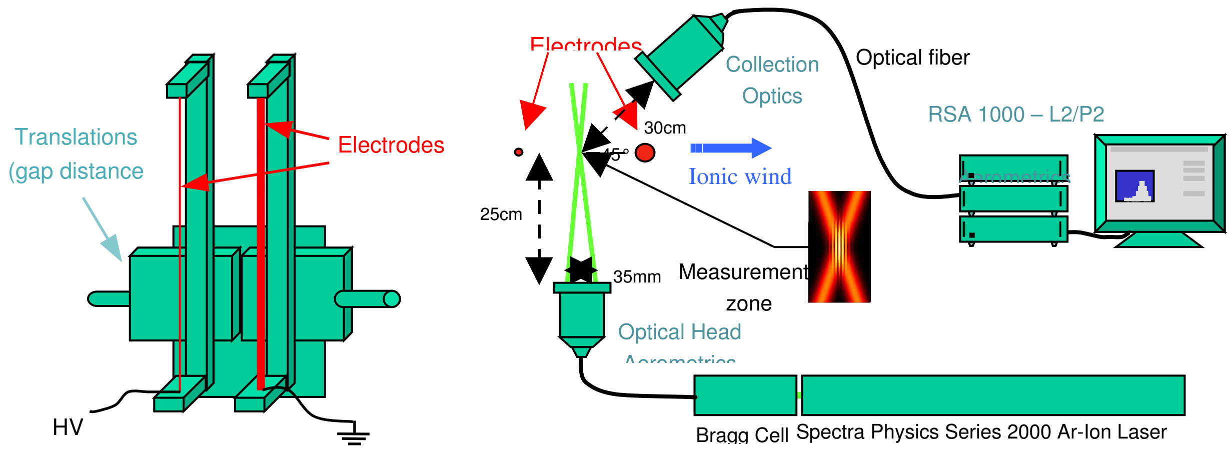

Fig. 1: Experimental setup

3. Experimental results

The thin and positively stressed electrode is surrounded by a uniform purple luminescent halo, characteristic of the emission of a corona discharge. When we increase the voltage, starting from 0, this emission appears at the same time as the current and increases with it up to the spark. The discharge remains a corona discharge until a spark appears above a certain voltage. Thus, we do not observe the behavior reported by Moreau *et al.* [8], who observed a "spot" regime up to 200 µA/m, a "streamer corona" regime from 200 to 800 µA/m and a "glow" from 800 to 2.5 mA/m. It should be noted however that Moreau *et al.* use a different configuration with a dielectric and a negatively biased cathode.

To observe possible high frequency current fluctuations, we measured the current through the circuit with a shunt and a LeCroy Wave Surfer 434 oscilloscope (350 MHz). In the negative discharge, we observed the well known Trichel pulses [10], of frequency proportional to the average current in the range 10 to 700 kHz in the range of current studied. Their duration is 300 ns and their amplitude a few mA. In the positive discharge, the behavior is different. The current is steady (current pulses of less than 0.15 mA at very low frequency between 1 and 10 Hz, independent of the applied voltage, are observed and are probably caused by internal characteristics of the power supply). We conclude that the positive discharge presents no current pulses. This result is again in disagreement with the results of Moreau *et al.* [11] for a configuration of two wires placed at the surface of a dielectric, hence suggesting the essential influence of the dielectric on the discharge electrodynamics.

As mentioned above, the corona is located in the vicinity of the stressed electrode, where the electric field and ionization rate are the highest. To examine the influence of the electrode material on the discharge and on the ionic wind, we made measurements with electrodes of copper, aluminum, steel, and zinc. First we considered pairs of electrodes of the same material, then combinations of materials. For each configuration we repeated the measurements of current-voltage characteristics several times at half-day intervals. First, no significant variation of the ionic wind with the humidity in ambient air was observed in the rage 1.0-1.5% of water vapor. Second, within experimental uncertainty, no difference was obtained for the current-voltage characteristics obtained with the different materials. We conclude that there is no effect of the nature of the material on the ionic wind in our case. However we observe that the maximum current reached before breakdown can vary by as much as a factor of two for different wires of a given material. We assume this can be explained by the state of the wire surface but we have not quantified this effect in the present study. For the rest of the parametric study presented here, we used copper electrodes.

Figure 2 shows the velocity as a function of the current for various gap distances. The wire diameters are fixed at 0.35 mm for the anode and 2.0 mm for the cathode. The fits show that in all cases the velocity varies with the square root of the current. This agrees with the literature [7]. That is, to increase the maximum flow velocity we have to maximize the current passing through the system. In the present experiments, the current was always limited by the appearance of a spark.

The gap between the two electrodes plays an important role. Figure 3 shows two graphs for a pair of wires of 0.2 and 2.0 mm of diameter. The circles in Figure 3 represent the maximum current reached just before the spark

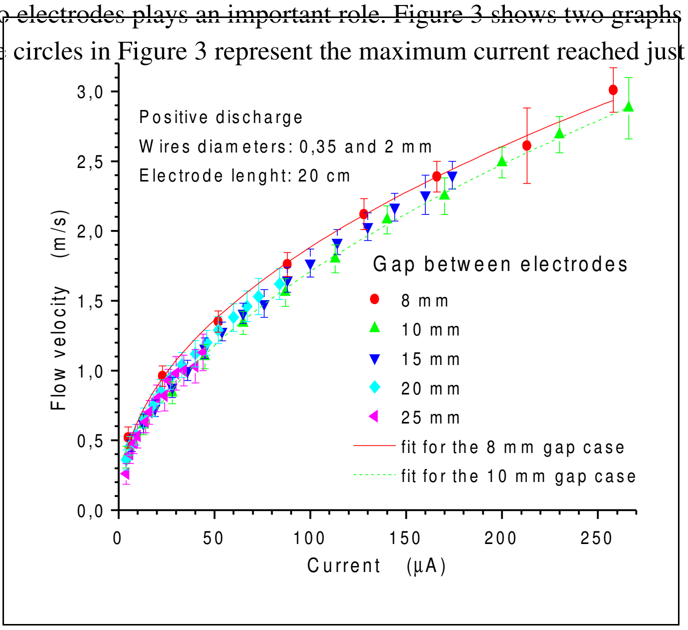

Fig. 2: Measured flow velocity as a function of the current and the gap distance. The fitted lines correspond to a power law x^a with a = 0.47 (solid line) and a = 0.53 (dotted line).

for each value of the gap distance. The highest currents are obtained for the smallest gap distance. Thus, to maximize the velocity, we have to minimize the gap distance. The squares in Figure 3 show the maximum voltage reached before breakdown divided by the gap distance, *i.e.* the maximum average electric field. The highest values are also obtained for the smallest gap distance. Based on theoretical expressions of Refs. [4] and [9], the electrodynamic force applied to the flow is proportional to the electric field. Figure 3 shows that on the range of gap distances studied, the highest force is obtained for the shortest gap distance.

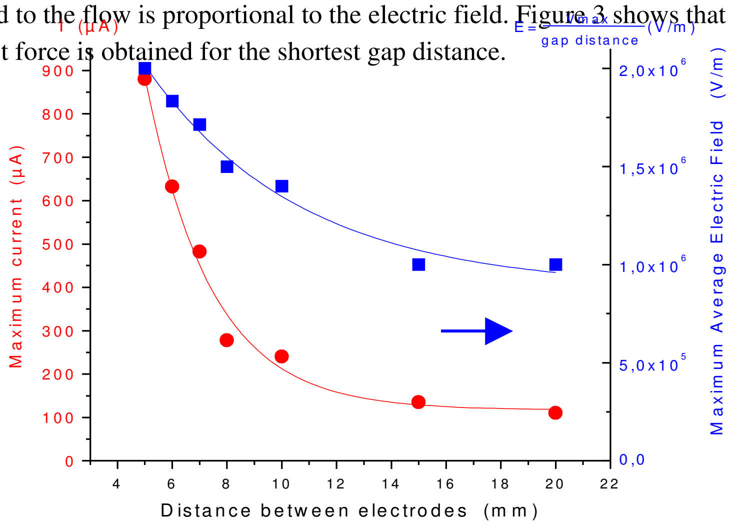

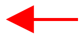

Fig. 3: Effect of the gap distance on the maximum current and electric field obtained before breakdown. The lines are exponential fits.

The other geometric parameters influencing the discharge are the wire diameters. In the vicinity of each wire, the electric field decreases inversely proportional to the distance to the wire. The thinner the wire, the greater the electric field at its surface. This has two consequences. If the two wires have the same diameter and if the mobilities of the positive and negative ions created at the electrodes are equal, then the drift ion currents created at both electrodes compensate and there is no net ionic wind. This was observed experimentally by Moreau *et al.* and confirmed in the present experiments. Increasing the dissymmetry between the two diameters favors one of the two ion currents. The other consequence is that if reducing the diameter of the small wire favors the ionization rate at its vicinity. Figure 4 shows that for fixed voltage the current is higher for a smaller diameter wire. In addition, the threshold of current increase occurs at a smaller voltage.

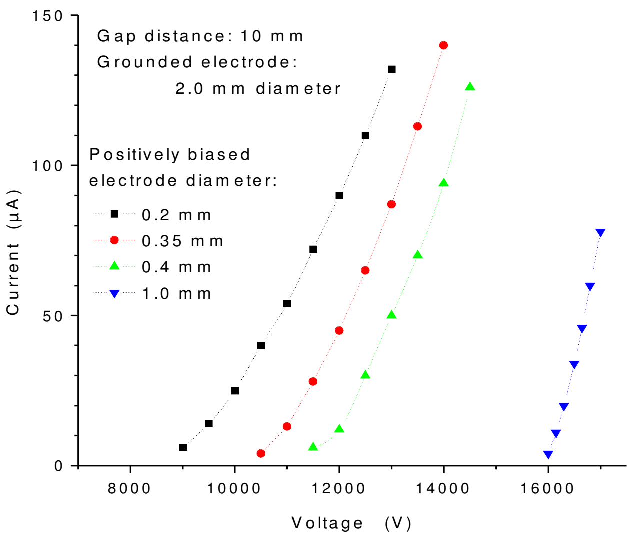

Fig. 4: Influence of the diameter of the thinnest wire on the current-voltage characteristic.

4. Model

Numerical simulations were made with FLUENT in a two-dimensional geometry for one configuration of our experiment: a gap distance of 10 mm, and wire diameters of 0.2 and 2.0 mm. Because experimentally we observe no fluctuations of the current or the voltage for the regimes investigated, all simulations are performed in steady state. The chemistry model contains 3 species: electrons, one species of positive ions and one species of negative ions. We solve simultaneously the steady-state continuity equations for electrons, positive ions, negative ions, the Poisson equation, and the Navier-Stokes equations with the Lorentz force term expressed as the product of the electric field by the net number density of ions:

$$= .(n_e \overrightarrow{u_e}) \quad S_{ion} \frac{E}{N} \quad S_{att} \frac{E}{N} \quad S_{e-ion} \frac{E}{N} \tag{1}$$

$$= .(n_+ \overrightarrow{u_+}) \quad S_{ion} \frac{E}{N} \quad S_{e-ion} \frac{E}{N} \quad S_{ion\_pos-ion\_neg} \frac{E}{N} \tag{2}$$

$$= .(n_- \overrightarrow{u_-}) \quad S_{att} \frac{E}{N} \quad S_{e-ion} \frac{E}{N} \quad S_{ion\_pos-ion\_neg} \frac{E}{N} \tag{3}$$

$$\Delta V = \frac{n_+ - n_- - n_e}{\varepsilon_o} \tag{4}$$

$$= .(\rho \vec{u}\vec{u}) \quad \vec{\ } p \quad e(n_+ \quad n_- \quad n_e)\vec{E} \quad \vec{\tau} \tag{5}$$

where n_e, n_+, n_- represent the density of electrons, positive ions and negative ions; S_{ion}, S_{att}, S_{e-ion}, $S_{ion\_pos-ion\_neg}$ the ionization, attachment, electron-ion recombination and positive-negative ion recombination rates, respectively. $\vec{u}$, $\overrightarrow{u_e}$, $\overrightarrow{u_+}$ and $\overrightarrow{u_-}$ are the velocities of the fluid, the electrons, the positive ions and the negative ions, respectively. V is the electric potential and $\vec{E}$ the electric field, and $\vec{\tau}$ the viscosity tensor. The drift-diffusion model is used:

$$n \ \overrightarrow{u} = \ \mu \ n \ \vec{E} - D \ \vec{\ } n \tag{6}$$

$$n_e \overrightarrow{u_e} = -\mu_e n_e \vec{E} - D_e \ \vec{\ } n_e \tag{7}$$

where μ_+, μ_-, μ_e, D_+, D_- and D_e respectively the mobilities and diffusion coefficients of positive ions, negative ions and electrons. The rates of ionization and attachment, and the diffusivity of electrons are taken from *Bolsig* [15] (see table 1). The fit of μ_e is taken from Chen *et al.* [12]:

$$\mu_e = 1.2365 E^{-0.2165} m^2 V^{-1} s^{-1} \tag{8}$$

Table 1: Bolsig data for airlike mixture [N2]:[O2] = 4:1

Red. Elect. field (V/cm/torr)	10	20	30	40	50	60	70	80	90	100	110	120	130	140	150	160	170	180	190	200
Diff. coeff. (torr.cm²/s)	583600	611400	751100	914600	1046000	1152000	1152000	1152000	1152000	1152000	1152000	1152000	1152000	1152000	1152000	1152000	1152000	1152000	1152000	1152000
Ionisation coeff. (1/cm/torr)	0	0.0001	0.0027	0.0156	0.0468	0.1102	0.1807	0.2835	0.4182	0.5672	0.7331	0.9087	1.106	1.296	1.526	1.748	1.974	2.197	2.461	2.676
Attach. coeff. (1/cm/torr)	0	0.0027	0.0088	0.0125	0.0136	0.0135	0.0128	0.012	0.0114	0.0106	0.0098	0.0092	0.0086	0.008	0.0076	0.0072	0.0068	0.0064	0.0061	0.0058

The ion-ion and the electron-ion recombination rates and the ion diffusion coefficient are taken as in Boeuf *et al.* [13]. The mobility of the positive and negative ions are taken equal to 2.5×10^{-4} and 2.7×10^{-4} $m^2V^{-1}s^{-1}$ respectively, following Ref.[12].

These equations are introduced into FLUENT by adjusting a generalized transport equation:

$$\frac{}{t} \rho\phi + \ .(\rho\vec{v}\phi - D \ \vec{\ } \phi) = S \tag{9}$$

in which we can define through modules the diffusion coefficient, the convective velocity, and the source terms. At the anode surface, the boundary conditions for the densities of electrons, positive ions and negative ions are: $\vec{n}.\vec{\nabla} n_e = 0$, $\vec{n}.\vec{\nabla} n_- = 0$ and $n_+ = 10^4 cm^{-3}$, with $\vec{n}$ the unit vector normal to the surface. At the cathode surface, the boundary conditions are $n_e = 10^3 cm^{-3}$, $n_- = 10^4 cm^{-3}$ and $\vec{n}.\vec{\nabla} n_+ = 0$. At the domain limit, $n_e = 10^3 cm^{-3}$, $n_- = n_+ = 10^4 cm^{-3}$, $\vec{E}.\vec{n} = 0$; the pressure is fixed at the atmospheric value and the velocities are normal to the boundary $\vec{n}.\vec{u} = 0$. The number densities of electrons and ions in ambient air are taken as referred in [14]: $n_e = 10^3 cm^{-3}$ and $n_- = n_+ = 10^4 cm^{-3}$. The 2D computational domain is as shown in Figure 5. Near the anode, the cell size is 1 µm x 1µm.

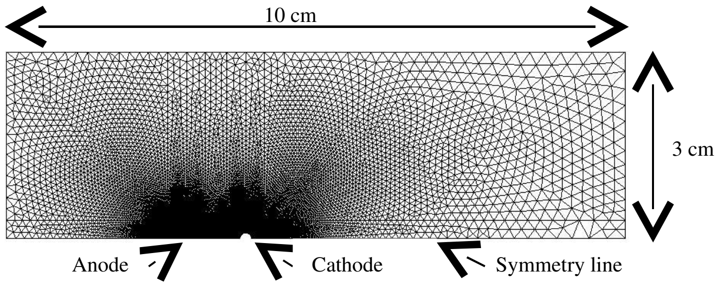

Fig 5: Computational domain

5. Numerical results

Figure 6 presents the simulated current-voltage characteristics for a pair of copper electrodes of diameter 0.2 and 2.0 mm separated by a distance of 10 mm and with a positively stressed electrode. The experiment and the simulation are in good agreement. The voltage threshold at which the discharge appears seems to be close. The general shape of the voltage dependence is similar: the simulation has the same behavior as the experiment.

Figures 7 and 8 present the measured and calculated velocities. The simulated velocities vary proportionally to the current to the power 0.70 instead of the measured value of 0.5. We tested some physical parameters of the discharge such as secondary electron emission. We find numerically that secondary electron emission at the cathode has no appreciable effect for values of the secondary electron emission coefficient γ less than 0.001. For higher values of γ, the simulated velocities present a sharp increase above a given voltage, in disagreement with the experimentally observed profile. Because the materials used in the present work all have γ values of less than 0.001 [5] we do not expect secondary emission to play a role here. Yet it would be interesting to find a material for which the coefficient is high enough to have an effect on the discharge and hence on the velocities.

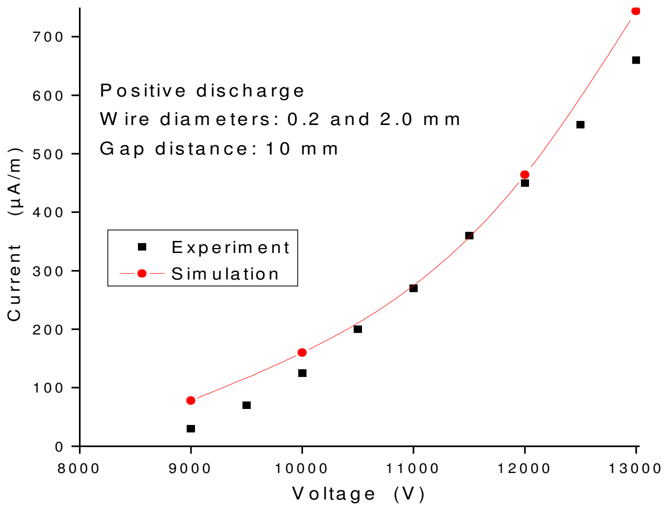

Fig. 6: Current-voltage characteristics. Comparison between experiment and simulation.

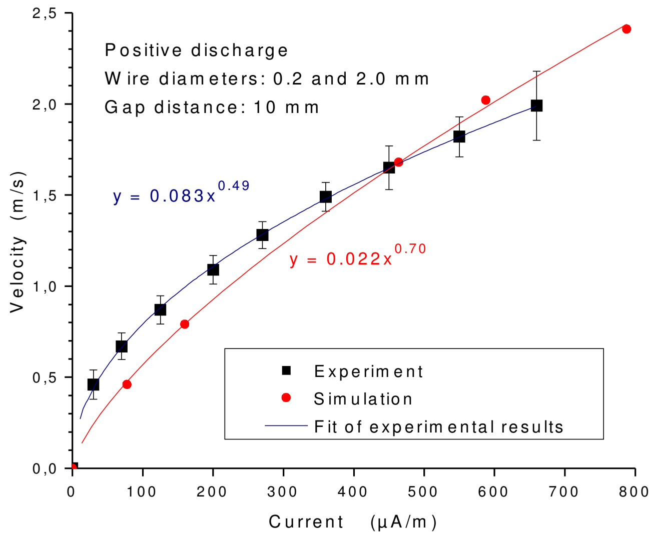

Fig. 7: Velocity as a function of the current. Comparison between experiment and simulation.

Figure 8 shows reasonable agreement between simulations and measurements of the velocity vs. the voltage. However the simulated velocity increases faster with voltage than the measured velocity. The velocity profile between the electrodes is plotted on Figure 9. It was not possible to make measurements closer to the anode. There is good agreement up to x = 7 mm and then the measurements have larger values. The difference can be explained as follows: the simulated profile corresponds to the stagnation streamline whereas the measured velocities are averaged over a small volume that includes particules going around the cathode.

The simulated number density profiles of charged species between the electrodes are presented on Figure 10. Because ionization is the highest at the vicinity of the anode and because of attachment to molecular oxygen, the electron density decreases rapidly away from the anode. The positive ion number density grows rapidly over the first few micrometers and reaches values that are much larger than the number density of negative ions and electrons over most of the inter-electrode space. Thus a positive unipolar region is created between the electrodes.

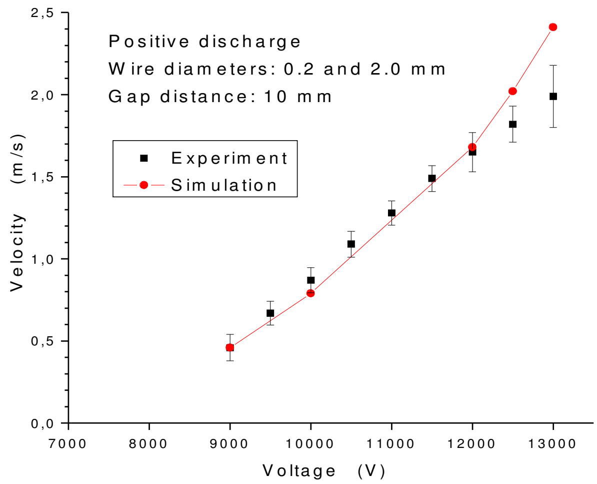

Fig 8: Velocity as a function of the voltage. Comparison between experiment and simulation.

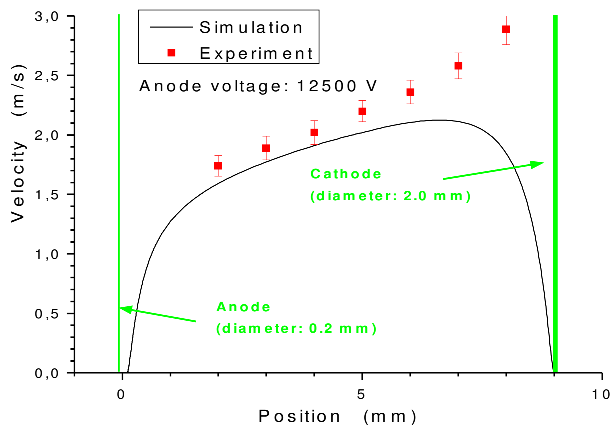

Fig. 9: Measured and simulated velocity profiles between the electrodes.

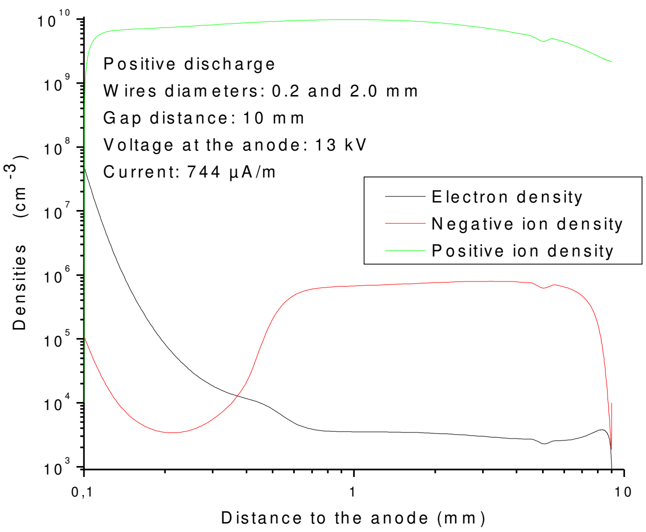

Fig. 10: Density profile for electrons, positive and negative ions

5. Conclusion

In this paper, we have presented a parametric study of the ionic wind produced by a corona discharge between two parallel wires. The parameters investigated are the diameter, material and polarity of the electrodes, the gap distance, the current, and the voltage. For the case of the positive corona discharge, steady current and voltage traces are observed. In contrast, the negative corona discharge exhibits current pulses (Trichel pulses). For the same absolute value of the stressed electrode's potential, the ionic wind velocity is always higher for the positive discharge. For the positive discharge the measured velocity varies with the square root of the current. The material of the electrodes and the ambient air humidity appear to have no effect on the velocity. The velocity increases with decreasing gap distance and increasing dissymmetry of the electrode diameters. The maximum velocity is always determined by the occurrence of a spark breakdown.

A model of the phenomenon is proposed. Comparisons of the measured and predicted velocity profiles are in reasonable agreement but the model must be improved to better fit the measurements. A detailed chemistry mechanism is currently being incorporated in the model. The calculated velocities vary with the current according to a power law with an exponent of 0.7 instead of the measured value of 0.5. The calculated current-voltage characteristics are in good agreement with the measured ones.

References

[1] Léger L., Moreau E., and Touchard G. Electrohydrodynamic airflow control along a flat plate by a DC surface corona discharge – velocity profile and wall pressure measurements. AIAA paper 2002-2833, in *1st Flow Control Conference*, St. Louis, Missouri, June 2002.

[2] Roth J.R., Sin H., and Madhan R.C.M. Flow re-attachment and acceleration by paraelectric and peristaltic electrohydrodynamic (EHD) effects. AIAA paper 2003-531, in *41st Aerospace Sciences Meeting & Exhibit*, Reno, Nevada, January 2003.

[3] Corke T.C., Mertz B., and Patel M.P. Plasma flow control optimized airfoil. AIAA paper 2006-1208, in *44th AIAA Aerospace Sciences Meeting & Exhibit*, Reno, Nevada, January 2006.

[4] Stuetzer O.M. Ion drag pressure generation. *Journal of Applied Physics*, 30, 7: 984-994, July 1959.

[5] Raizer Y.P. Gas Discharge Physics. In *Springer*, 1997.

[6] Matéo-Vélez J.C. Modélisation et simulation numérique de la génération de plasma dans les décharges couronnes et son intéraction avec l'aérodynamique. PhD thesis, École Nationale Supérieure de l'Aéronautique et de l'Espace, Dec. 2006.

[7] Robinson M. Movement of air in the electric wind of the corona discharge. *Transactions of the American Institute of Electrical Engineer, Part1 Communication and Electronic*, 80: 143-150, 1961.

[8] Léger L., Moreau E., Touchard G., Effect of a DC corona electrical discharge on the airflow along a flat plate. *IEEE Transactions on Industry Applications*, 38, 6, 1478-1485, November-December 2002.

[9] Lacoste D.A., Pai D., Laux C.O. Ion wind effect in a positive DC corona discharge in atmospheric pressure air. AIAA paper 2004-0354, in *42nd Aerospace Sciences Meeting & Exhibit*, Reno, Nevada, January 2004.

[10] Ress T., Paillol J. The role of the field-effect emission in trichel pulse development in air at atmospheric pressure. *Journal. of Physics D, Applied Physics, 30*: 3115-3122,1997.

[11] Moreau E., Artana G., Touchard G. Surface corona discharge along an insulating flat plate in air applied to electrohydrodynamical airflow control: electrical properties. In *Electrostatics 2003, 178, IOP Publishing Ltd*, Bristol-Philadelphia, pages 285-290, 2004.

[12] Chen J. and Davidson J. Electron density and energy distribution in the positive DC corona: interpretation for corona-enhanced chemical reactions. *Plasma Chem. & Plasma Processing,* 22, 2: 199-224, June 2002.

[13] Boeuf J.P., Lagmich Y., Callegari T., Pitchford L.C. Electrohydrodynamic force and acceleration in surface discharges. AIAA paper 2006-3574, in *37th AIAA Plasmadynamics and Lasers Conference*, San Francisco, California, June 2006.

[14] Rühling F., Heilbronner F., Ortéga P. Discharge inception under impulse voltage: influence of lab air density and resulting charge-voltage relation. In *13th International Symposium on High Voltage Engineering*, Netherlands, 2003.

[15] CPAT & Kinema Software, http://www.siglo-kinema.com/bolsig.htm.

This page has been purposely left blank